Integrated fault-tolerant control for a 3-DOF helicopter with actuator faults and saturation

Jianglin Lan[1], Ron J. Patton[1,*], Xiaoyuan Zhu[2]

[1]School of Engineering and Computer Science, University of Hull, Cottingham Road, Hull HU6 7RX, UK
[2]Merchant Marine College, Shanghai Maritime University, 1550 Haigang Ave, Shanghai 201306, China
[*]r.j.patton@hull.ac.uk

Abstract: This paper proposes a fault estimation (FE) based fault-tolerant control (FTC) strategy to maintain system reliability and achieve desirable control performance for a 3-DOF helicopter system with both actuator drift and oscillation faults and saturation. The effects of the faults and saturation are combined into a composite non-differentiable actuator fault function, which is approximated by a differentiable function and estimated together with the system state using a nonlinear unknown input observer. An adaptive sliding mode controller based on the estimates is developed to compensate the effects of the faults and saturation. Taking into account the bi-directional robustness interactions between the FE and FTC functions, an integrated design approach is proposed to obtain the observer and controller gains in a single-step so as to achieve robust overall FTC system performance. In fault-free cases, the proposed strategy can be considered as a new approach for anti-windup control to compensate the effect of input saturation. Comparative simulations are provided to verify the effectiveness of the proposed design under different actuator fault scenarios.

1. Introduction

Reliability is critical for flight control systems, since in practical operations they may suffer from certain system faults (e.g., actuator fault, sensor fault and component fault) that prevent them from achieving planning tasks and degrade their system performance. In order to maintain robust flight system performance, fault estimation (FE) and fault-tolerant control (FTC) designs have attracted significant attention, see [1, 2] and the references therein. FE is designed to estimate the fault and corresponding fault compensation is then performed through the FTC controller by making use of the estimate [3].

Unmanned aerial vehicles (UAVs) have numerous applications in military and civilian domains, due to their small size and features of long air hovering, vertical take-off and landing capability, low-speed/-altitude and flexible flight [4]. The control designs for UAVs have been researched extensively, see for example [5–8]. Considering reliability and safety, FE and FTC designs for UAV control systems have also attracted lots of attention, see [9–13] and the references therein.

The implementation of FTC of most UAVs becomes very challenging due to the lack of actuator or sensor (hardware redundancy) in these systems. An exception to this for UAVs is the actuator redundancy that exists in hexrotor and octorotor systems. However, in this study all forms of

hardware redundancy are excluded as a deliberate exercise to test the potential of FE-based FTC. The Quanser 3-DOF helicopter model with twin rotors [14] is considered in this paper. This model has been used by many researchers as a benchmark case study which is representative of the rigid body dynamics of a full-size tandem rotor transport and rescue helicopter. Studies are focused on the use of this system to verify control designs [7, 15–17]. It is interesting to note that this system can also be representative of a rigid body UAV system. There is no hardware redundancy and the FTC must be based fully on the analytical or functional redundancy concept, i.e. using combined fault and state estimation.

Many FE/FTC designs for the Quanser 3-DOF helicopter model have also been published [18–23]. [18] proposes an adaptive sliding mode observer (SMO) for actuator fault estimation for a Lipschitz nonlinear helicopter model without uncertainty and external disturbance. In their work the faults are estimated with ultimately bounded errors and FTC is out of its scope. [19] presents an improved robust model predictive FTC design considering a linear 3-DOF helicopter system with uncertainty, disturbance and an actuator fault. However, model predictive control involves online optimisation and their work does not include FE. [20–22] describe adaptive FTCs for uncertain nonlinear 3-DOF helicopter systems, also excluding FE. These methods cannot offer explicit fault information (location, magnitude and time occurrence) that is useful for subsequent system maintenance. An FE-based FTC output tracking strategy is developed in [23] for a linearised 3-DOF helicopter with perturbations and oscillatory and drift actuator faults. In their work FE is obtained by a higher order SMO and FTC is achieved by a backstepping sliding mode controller based on system decomposition. The main drawbacks of their work are: 1) It requires the system output derivatives which are difficult to obtain in real implementation, and 2) it designs the FE observer and FTC controller separately without considering the mutual influences between the estimation and control.

Although an acceptable control performance can be achieved by the separated FE/FTC design for line systems without uncertainty, it is difficult or impossible to be achieved in the presence of uncertainty and nonlinearity. It is described in [24] that the occurrence of inevitable system uncertainty leads to an existence of bi-directional robustness interactions between the FE and FTC functions within a closed-loop system scheme, which gives rise to a requirement of an integration of FE and FTC to achieve robust FTC performance. [24] also proposes an effective integrated FE/FTC strategy for uncertain linear systems using an unknown input observer (UIO) and a single-step linear matrix inequality (LMI) formulation. Their approach is further extended by [25] for Lipschitz nonlinear systems with actuator/sensor faults. However, neither of these works considers the effects of actuator saturation.

Actuator saturation is a function of flight system design in most real aircraft systems and for full-size aircraft it is always taken into account. It is thus necessary to include a study of the effect of actuator saturation on the performance of an FTC scheme for a UAV. Actuator saturation problems for 3-DOF helicopters have been considered in [26] using an inversion-based control approach, and by [27] with an anti-windup compensator. However, they do not pay attention to actuator faults.

This work aims to extend the strategy in [25] for stabilising the elevation and pitch motions of an uncertain nonlinear 3-DOF helicopter system with both actuator faults and saturation. Compared with the existing works, the main contributions of this paper are in three aspects:

1) An uncertain nonlinear 3-DOF helicopter with both actuator faults and saturation is considered. The actuator faults and the saturation are combined into a composite fault function which are non-differentiable. The composite fault function is further approximated by a differentiable

function with a sufficiently small error and treated as a new system state that estimated by a non-linear unknown input observer (NUIO). Unlike the adaptive SMO [18] and higher order SMO [23] FE methods, the proposed NUIO can achieve asymptotic estimation of the faults with no need for system output derivatives.

2) An adaptive sliding mode FTC controller is proposed to compensate the effects of the actuator faults and saturation and stabilise the elevation and pitch motions of the 3-DOF helicopter. Sliding mode control (SMC) is known as a robust control method, since once sliding motion is reached the system is insensitive to any matched perturbation (within the range space spanned by the control input) [28]. Moreover, the adaptive method is incorporated with the SMC to avoid the requirement of *a priori* knowledge of the perturbation bounds. Compared with model predictive FTC [19], adaptive FTCs [20–22], and backstepping sliding mode FTC [23], the proposed FTC is easier to design and implement without online optimisation and system decomposition, and the FE observer and FTC controller gains are obtained using a single-step LMI formulation.

3) In the absence of actuator faults, the proposed integrated FTC design reverts to a new anti-windup control method for compensating the input saturation effect to recover the non-saturated system performance.

The remainder of this paper is organized as follows. Section 2 models the 3-DOF helicopter system and formulates the control problem. Section 3 proposes a NUIO for FE and Section 4 develops an adaptive sliding mode FTC controller. The synthesis of the observer and controller is presented in Section 5. Simulation results are provided in Section 6 and conclusions are drawn in Section 7.

Notation: The symbol $\mathbb{R}$ denotes the set of real numbers; $|\cdot|$ denotes the absolute value; $\|\cdot\|_p$ denotes the $p-$norm in the Euclidean space, and $\|\cdot\|$ and $\|\cdot\|_\infty$ represent the 2-norm and $\infty-$norm, respectively; $\mathcal{L}_2[0,\infty)$ denotes the 2-norm space; $\mathrm{He}(W_0) = W_0 + W_0^\top$, and $\star$ denotes the transpose of the matrix element on its symmetric position in a matrix; I_p denotes a $p \times p$ identity matrix; $\kappa_{m \times n}$ denotes a $m \times n$ matrix whose elements are all equal to a constant κ; $\mathrm{sign}(\varpi)$ denotes the signum function of the variable ϖ defined by $\mathrm{sign}(\varpi) = \varpi/\|\varpi\|$, and if $\varpi = 0$, $\mathrm{sign}(\varpi) = 0$.

2. Problem formulation
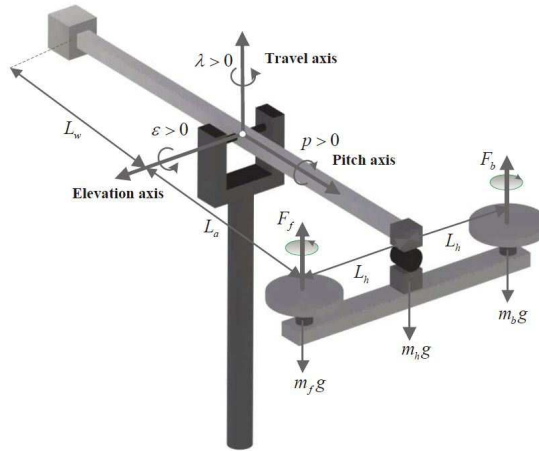
Fig. 1. *A free body diagram of the Quanser 3-DOF helicopter [16]*

Table 1 Definitions of the physical parameters

Parameter	Physical meaning
ε	Elevation angle
p	Pitch angle
F_f, F_b	Control voltages of the front and back motors
J_ε, J_p	Moments of inertia of elevation and pitch axes
K_f	Propeller force-thrust constant
m_h	Mass of the helicopter
L_a	Distance within the travel axis and the helicopter body
L_h	Distance between the pitch axis and each motor
g	Gravity constant
w_ε, w_p	Unknown external disturbances belong to $\mathcal{L}_2[0, \infty)$

This work considers the elevation and pitch motions of the Quanser 3-DOF helicopter (Fig. 1) with the model [16]

$$
\begin{aligned}
J_\varepsilon \ddot{\varepsilon} &= K_f L_a \cos(p)\left(F_f + F_b\right) - m_h g L_a \sin(\varepsilon) + w_\varepsilon, \\
J_p \ddot{p} &= K_f L_h \left(F_f - F_b\right) + w_p,
\end{aligned}
\tag{1}
$$

where the physical parameters are defined in Table 1.

Define the system state vector as $x = [x_1\ x_2\ x_3\ x_4]^\top = [\varepsilon\ p\ \dot{\varepsilon}\ \dot{p}]^\top$, the input vector as $u = [u_1\ u_2]^\top = [F_f\ F_b]^\top$, and the output vector as $y = [\varepsilon\ p\ \dot{\varepsilon}\ \dot{p}]^\top$. Assume that the front and back motors suffer from saturation and unknown actuator faults f_{a1} and f_{a2}, respectively. The actuator faults may be oscillatory faults [29] or drift faults [23] acting on flight or helicopter control systems. Without loss of generality, f_{a1} and f_{a2} are assumed to have first-order time derivatives $\dot{f}_{a1}$ and $\dot{f}_{a2}$, respectively. Moreover, f_{a1}, f_{a2}, $\dot{f}_{a1}$, and $\dot{f}_{a2}$ are bounded and belong to $\mathcal{L}_2[0, \infty)$. Hence, the control inputs applied to the helicopter (see Fig. 2) can be represented as

$$
u_i = \text{sat}(u_{0i} + f_{ai}), \ i = 1, 2,
$$

where u_{0i} is the designed control input and $\text{sat}(\cdot)$ is a saturation function defined by

$$
\text{sat}(v) = \left\{ \begin{array}{ll} \text{sign}(v)\bar{u}, & |v| \geq \bar{u} \\ v, & |v| < \bar{u} \end{array} \right.,
$$

with v the input to the actuator and $\bar{u}$ the maximum voltage of the actuator.
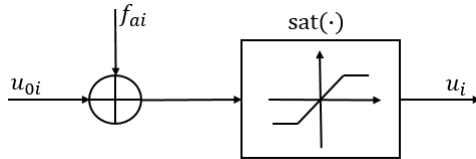
Fig. 2. *The actuator model with both fault and saturation*

The control input u of the system (1) can then be rearranged into

$$
u = u_0 + f_0,
\tag{2}
$$

where $u_0 = [u_{01} \ u_{02}]^\top$ is the designed control input vector and $f_0 = [f_{01} \ f_{02}]^\top$ is the composite actuator fault vector with $f_{0i} = \text{sat}(u_{0i} + f_{ai}) - u_{0i}$, $i = 1, 2$.

Remark 1. In real operations, the helicopter actuators may suffer from both stuck and partial loss of effectiveness faults [30, 31]. For this case, the control inputs applied to the helicopter are represented by

$$u_i = \text{sat}(\theta_i u_{0i} + u_{si}), \ i = 1, 2, \tag{3}$$

where θ_i is the partial loss of effectiveness fault taking values within the sector $[0, 1]$ and u_{si} is the stuck fault. Assume that both θ_i and u_{si} are unknown bounded and differentiable time-varying functions. The actuator model (3) can be rearranged into

$$u = u_0 + f_0, \tag{4}$$

where $u_0 = [u_{01} \ u_{02}]^\top$ is the designed control input vector and $f_0 = [f_{01} \ f_{02}]^\top$ is the composite actuator fault vector with $f_{0i} = \text{sat}(\theta_i u_{0i} + u_{si}) - u_{0i}$, $i = 1, 2$. Since (4) and (2) are in the same form, the FE and FTC strategies proposed in this paper can be directly applied to the estimation and compensation of the total effect of saturation and stuck and partial loss of effectiveness faults.

According to the aforementioned definitions a state-space model of (1) is given as

$$\begin{aligned}
\dot{x} &= Ax + B(u_0 + f_0) + g(x) + Dd, \\
y &= Cx,
\end{aligned} \tag{5}$$

with $d = [d_1 \ d_2]^\top$ and

$$A = \begin{bmatrix} 0 & 0 & 1 & 0 \\ 0 & 0 & 0 & 1 \\ 0 & 0 & 0 & 0 \\ 0 & 0 & 0 & 0 \end{bmatrix}, \ B = \begin{bmatrix} 0 & 0 \\ 0 & 0 \\ b_1 & b_1 \\ b_2 & -b_2 \end{bmatrix},$$

$$D = \begin{bmatrix} 0 & 0 \\ 0 & 0 \\ 1 & 0 \\ 0 & 1 \end{bmatrix}, \ g(x) = \begin{bmatrix} 0 \\ 0 \\ g_1(x) \\ 0 \end{bmatrix}, \ C = I_4,$$

where $d_1 = w_\varepsilon/J_\varepsilon + b_1(\cos(x_2)-1)(u_{01} + f_{01} + u_{02} + f_{02})$, $d_2 = w_p/J_p$, $g_1(x) = -m_h g L_a \sin(x_1)/J_\varepsilon$, $b_1 = K_f L_a/J_\varepsilon$, and $b_2 = K_f L_h/J_p$. d is a bounded lumped uncertainty including external disturbances and the system uncertainty $b_1(\cos(x_2) - 1)(u_{01} + f_{01} + u_{02} + f_{02})$. It is verified that the system (5) is observable and controllable. The following assumption is made throughout the paper.

Assumption 1. The nonlinear function $g(x)$ satisfies the Lipschitz constraint

$$\|g(x_t) - g(x)\| \leq L_f \|x_t - x\|, \ \forall \, x, x_t \in \mathbb{R}^4,$$

where L_f is the Lipschitz constant independent of x.

Remark 2. It is seen from (5) that the nonlinear function $g(x)$ satisfies the Lipschitz constraint in Assumption 1 with $L_f = m_h g L_a/J_\varepsilon$.

The presence of actuator faults and saturation can affect the helicopter system stability and prevent it from performing prescribed tasks. This paper aims to stabilise the elevation and pitch angles of the system (5) through an FTC strategy involving: 1) The design of an observer to estimate the system state and the composite actuator fault; 2) The design of an FTC controller based on the estimates to compensate the faults and saturation effect to ensure system stability.

5

3. FE observer design

This section describes an observer design for estimating the system state x and composite actuator fault f_0. A NUIO adopted from [25] is used to achieve the estimation, in which f_0 is extended as a new system state and must be differentiable.

It can be seen from (2) that f_0 is a function of the designed control input u_0 and the saturation function $\mathrm{sat}(v)$. In this paper u_0 is designed in Section 4 as a state-feedback controller that is differentiable. However, the saturation function $\mathrm{sat}(v)$ is known to be non-differentiable. Therefore, f_0 is non-differentiable which cannot be treated as a new system state. To overcome this, a differentiable approximation of f_0 needs to be attained before designing the NUIO.

3.1. Differentiable approximation of f_0

The above analysis implies that if the saturation function $\mathrm{sat}(v)$ can be approximated by a differentiable function $\overline{\mathrm{sat}}(v)$, then f_0 is modelled as a new function consisting of a differentiable function of u_0 and $\overline{\mathrm{sat}}(v)$ and the approximation error which can be combined into the uncertainty term. In this way, a differentiable approximation of f_0 is attained.

The saturation function $\mathrm{sat}(v)$ is approximated by a differentiable function $\overline{\mathrm{sat}}(v)$ modified from [32] with the form of

$$\overline{\mathrm{sat}}(v) = \begin{cases} v, & 0 \leq |v| \leq \bar{u} \\ v - \frac{[v - \bar{u}\,\mathrm{sign}(v)]^2 \mathrm{sign}(v)}{2\epsilon_0}, & \bar{u} \leq |v| \leq \bar{u} + \epsilon_0 \\ (\bar{u} + \frac{\epsilon_0}{2})\mathrm{sign}(v), & |v| \geq \bar{u} + \epsilon_0 \end{cases}, \tag{6}$$

where ϵ_0 is a positive constant.

It can be shown that the function $\overline{\mathrm{sat}}(v)$ satisfies continuity across $|v| = \bar{u}$ as well as $|v| = \bar{u} + \epsilon_0$. Furthermore, the left and right derivatives of $\overline{\mathrm{sat}}(v)$ with respect to v at the above boundaries are equal. It follows that $\overline{\mathrm{sat}}(v)$ is differentiable. Moreover, it is bounded uniformly in ϵ_0 on any bounded interval of ϵ_0, and $|\overline{\mathrm{sat}}(v) - \mathrm{sat}(v)| \leq \epsilon_0/2$ and $0 \leq d\overline{\mathrm{sat}}(v)/dv \leq 1$ for all $v \in \mathbb{R}$. Hence, the approximation error of $\mathrm{sat}(v)$ is small as long as ϵ_0 is selected to be sufficiently small.

According to (6), the control input (2) can be further modelled as

$$u = u_0 + f + \Delta u, \tag{7}$$

where $f = [f_1\ f_2]^\top$ and $\Delta u = [\Delta u_1\ \Delta u_2]^\top$, with $f_i = \overline{\mathrm{sat}}(u_{0i} + f_{ai}) - u_{0i}$ and $\Delta u_i = \mathrm{sat}(u_{0i} + f_{ai}) - \overline{\mathrm{sat}}(u_{0i} + f_{ai})$, $i = 1, 2$.

Now the composite actuator fault f is differentiable, which can then be augmented as a new system state of the system (5) with input (7).

3.2. Observer design

The augmented system takes the form of

$$\begin{aligned} \dot{\bar{x}} &= \bar{A}\bar{x} + \bar{g}(A_0\bar{x}) + \bar{B}u_0 + \bar{D}\bar{d}, \\ y &= \bar{C}\bar{x}, \end{aligned} \tag{8}$$

6

where $\bar{x} = [x^\top f^\top]^\top$, $\bar{d} = [\tilde{d}^\top \dot{f}^\top]^\top$, $\tilde{d} = d + B_2 \Delta u$, $B_2 = [0 \ I_2]B$, $A_0 = [I_4 \ 0]$, and

$$\bar{A} = \begin{bmatrix} A & B \\ 0 & 0 \end{bmatrix}, \ \bar{B} = \begin{bmatrix} B \\ 0 \end{bmatrix}, \ \bar{D} = \begin{bmatrix} D & 0 \\ 0 & I_2 \end{bmatrix},$$

$$\bar{C} = [C \ 0], \ \bar{g}(A_0\bar{x}) = \begin{bmatrix} g(A_0\bar{x}) \\ 0 \end{bmatrix}.$$

It can be verified that the system (8) is observable since the pair (A, C) is observable and CB is of full rank for the considered helicopter system (5).

A NUIO is designed to estimate the augmented state $\bar{x}$ with the form of

$$
\begin{aligned}
\dot{z} &= Mz + Gu_0 + N\bar{g}(A_0\hat{\bar{x}}) + Ly, \\
\hat{\bar{x}} &= z + Hy,
\end{aligned}
\tag{9}
$$

where $z \in \mathbb{R}^6$ is the observer system state and $\hat{\bar{x}} \in \mathbb{R}^6$ is the estimate of $\bar{x}$. The matrices $M \in \mathbb{R}^{6\times6}$, $G \in \mathbb{R}^{6\times2}$, $N \in \mathbb{R}^{6\times6}$, $L \in \mathbb{R}^{6\times4}$, and $H \in \mathbb{R}^{6\times4}$ are to be designed. The estimates of x and f are $\hat{x} = [I_4 \ 0]\hat{\bar{x}}$ and $[0 \ I_2]\hat{\bar{x}}$, respectively.

Define the estimation error as $e = \bar{x} - \hat{\bar{x}}$, then

$$
\begin{aligned}
\dot{e} &= (\Xi\bar{A} - L_1\bar{C})e + (\Xi\bar{A} - L_1\bar{C} - M)z + (\Xi\bar{B} - G)u_0 \\
&\quad + [(\Xi\bar{A} - L_1\bar{C})H - L_2]y + \Xi\bar{g}(A_0\bar{x}) - N\bar{g}(A_0\hat{\bar{x}}) \\
&\quad + \Xi\bar{D}\bar{d},
\end{aligned}
\tag{10}
$$

where $\Xi = I_6 - H\bar{C}$ and $L = L_1 + L_2$. The matrices M, N, G, and L_2 are defined as

$$M = \Xi\bar{A} - L_1\bar{C}, \ N = \Xi, \ G = \Xi\bar{B}, \ L_2 = (\Xi\bar{A} - L_1\bar{C})H. \tag{11}$$

Note that the design matrices M, N, G, and L_2 can be calculated directly from (11) by substituting the matrices L_1 and H attained later through the LMIs in Theorems 2 - 4 in Section 5.

Substituting (11) into (10) gives

$$\dot{e} = (\Xi\bar{A} - L_1\bar{C})e + \Xi\Delta\bar{g} + \Xi\bar{D}\bar{d}, \tag{12}$$

where $\Delta\bar{g} = \bar{g}(A_0\bar{x}) - \bar{g}(A_0\hat{\bar{x}})$.

A sufficient condition for the existence of a robust NUIO (9) is given in Theorem 1.

Theorem 1. There exists a robust NUIO (9) if the error system (12) is robustly asymptotically stable.

Proof. If (12) is robustly asymptotically stable, then by (11), the error system (10) is also robustly asymptotically stable. Therefore, it holds that $\lim_{t\to\infty} e(t) = 0$ in the presence of uncertainty and disturbance. $\square$

According to Theorem 1, the solvability of (9) now becomes an problem of designing the matrices L_1 and H such that (12) is robustly asymptotically stable.

4. FTC controller design

This section presents the design of an adaptive system for FTC based on state and fault estimation. The FTC function is to compensate the estimated effects of the actuator faults and saturation and also stabilise the system state of (5). Since in the system (5) the state vector x are unavailable and the measured output vector y may have noise, thus it is appropriate to use the concept of SMC with adaption based on the combined state and fault estimation.

Recall that the general aim of SMC is to achieve robust insensitivity to matched uncertainty acting within the control channels, using a combination of linear and switched feedback. The SMC must be designed to reach a sliding surface and the switching operation designed to keep the system motion in the sliding manifold.

So in this SMC, the sliding surface for the system (5) is a function of the system state estimates as follows.

$$s = N_1 \hat{x} = 0, \tag{13}$$

where $s \in \mathbb{R}^2$, $\hat{x}$ is the system state estimate obtained through the observer (9) (i.e., $\hat{x} = [I_4 \ 0]\hat{\bar{x}}$), and $N_1 = B^\dagger - Y_1(I_4 - BB^\dagger)$ with $B^\dagger = (B^\top B)^{-1}B^\top$ and a design matrix $Y_1 \in \mathbb{R}^{2\times 4}$.

The first step of the SMC design is to establish the reachability of $\hat{x}$ to the sliding surface (13). Differentiating s with respect to time gives

$$\dot{s} = N_1 Ax + u_0 + f + N_1 g(x) + N_1 D\tilde{d} - N_1 \dot{e}_x, \tag{14}$$

where e_x is the estimation error of x defined as $e_x = x - \hat{x}$.

An FTC controller for the system (5) with (7) is designed as

$$u_0 = u_l + u_n, \tag{15}$$

where u_l is the linear feedback component given by $u_l = -K\hat{\bar{x}}$ with a design matrix $K = [K_x \ K_f]$. $K_x \in \mathbb{R}^{2\times 4}$ is to be determined while K_f is chosen as $K_f = I_2$. The nonlinear component u_n is $u_n = -\rho\overline{\text{sign}}(s, \theta_0)$, where ρ is a design scalar function. The smooth function $\overline{\text{sign}}(s, \theta_0)$ is defined as $\overline{\text{sign}}(s, \theta_0) = \frac{s}{\|s\|+\theta_0}$ [28], with a sufficiently small positive constant θ_0. It is a differentiable approximation of $\text{sign}(s)$ ensuring that the control function u_0 is also differentiable. Define the approximation error as $\Delta_{\text{sign}} = \text{sign}(s) - \overline{\text{sign}}(s, \theta_0)$, then it can be verified that $\|\Delta_{\text{sign}}\| \leq \frac{1}{\|s\|/\theta_0+1} \leq 1$ and for $\|s\| \neq 0$, $\|\Delta_{\text{sign}}\|$ is small by selecting a sufficiently small θ_0.

Consider the following Lyapunov function

$$V_s = \frac{1}{2}s^\top s.$$

The time derivative of V_s along (14) is

$$\begin{aligned}
\dot{V}_s &= s^\top \left[(N_1 A - K_x)x + \Delta_e - \rho\overline{\text{sign}}(s, \theta_0) \right] \\
&= s^\top \left[(N_1 A - K_x)x + \Delta_e + \rho\Delta_{\text{sign}} - \rho\text{sign}(s) \right] \\
&\leq (\omega\|x\| + \eta - \rho) \|s\|, \tag{16}
\end{aligned}$$

where $\Delta_e = K_x e_x + e_f + N_1 g(x) + N_1 D\tilde{d} + N_1 \dot{e}_x$, $e_f = f - \hat{f}$, and $\omega = \|N_1 A - K_x\|$. η is an unknown positive constant satisfying $\eta \geq \|\Delta_e\| + \|\rho\Delta_{\text{sign}}\|$.

Define $\rho = \hat{\eta} + \varphi + \epsilon$, where φ and ϵ are positive design constants. The scalar $\hat{\eta}$ is the estimate of η defined by

$$\dot{\hat{\eta}} = \sigma \|s\|, \ \hat{\eta}(0) \geq 0, \tag{17}$$

with a positive design constant σ.

Define the estimation error of η as $\tilde{\eta} = \eta - \hat{\eta}$. Consider a Lyapunov function

$$V = V_s + \frac{1}{2\sigma}\tilde{\eta}^2.$$

It follows from (16) and (17) that

$$
\begin{aligned}
\dot{V} &= s^\top \dot{s} - \frac{1}{\sigma}\tilde{\eta}\dot{\hat{\eta}} \\
&\leq (\omega\|x\| + \eta - \rho)\|s\| - \tilde{\eta}\|s\| \\
&= -\epsilon\|s\| - (\varphi - \omega\|x\|)\|s\|.
\end{aligned}
\tag{18}
$$

By choosing $\varphi > \omega\phi$ with a design positive scalar ϕ, then it follows from (18) that $\dot{V} \leq 0$ in the subset $\Omega = \{x : \|x\| \leq \phi\}$. On the one hand, $\dot{V} = 0$ holds only when $s = 0$. On the other hand, since $V \geq 0$, then if $\dot{V} < 0$, $\lim_{t\to\infty} V(t) = 0$. Hence, if $x(0) \in \Omega$, then $\dot{V} \leq 0$ leads to $\lim_{t\to\infty} s(t) = 0$ and all the signals (including $\hat{\eta}$) in the dynamics (14) are bounded. This proves that s is asymptotic convergence, i.e., converges to zero in infinite time.

However, it can be seen from (17) that $\hat{\eta}$ is non-negative and increasing. Thus, $\hat{\eta}$ tends to infinity if s is asymptotically convergent, which leads to a contradiction. So the sliding surface $s(t) = 0$ is reached in finite time t_r, provided that $x(0) \in \Omega$.

Remark 3. After finite time t_r, the system dynamics reach the sliding surface and remain there and converge to the origin asymptotically, as proved in Theorems 2 - 4. Therefore, for any given initial state vector $x(0)$, ϕ can be designed such that $\phi \geq \|x(0)\|$. This means that the attraction domain (set of admissible initial states) of the proposed FTC design is $\Omega_1 = \{x(0) : \|x(0)\| \leq \max(\|x(0)\|), \forall \ |x_i(0)| \leq \bar{x}_i, \ i = 1, 2, 3, 4\}$, where $\bar{x}_i$ is the maximum absolute value of x_i determined according to its physical limits. For the 3-DOF helicopter system example studied in this paper, the physical limits are those of the pitch and elevation angles. It should be noted that after choosing ϕ, another control design constant φ should be selected such that $\varphi > \omega\phi$.

Consider next the system stability analysis corresponding to the sliding mode. After t_r the system has already reached the sliding mode with the equivalent control input

$$u_{eq} = -\left[N_1 A x + N_1 g(x) + N_1 D\tilde{d}\right] + u_l. \tag{19}$$

Substituting (19) into (5) gives the equivalent closed-loop system

$$\dot{x} = (\Theta A - B K_x)x + B K e + \Theta g(x) + \Theta D\tilde{d}, \tag{20}$$

where $\Theta = I_4 - B N_1$.

Therefore, the system (5) is maintained on the sliding mode with the equivalent control (19) by designing K_x such that (20) is stable. The closed-loop system (20) contains the uncertainty $\tilde{d}$ and nonlinearity $g(x)$, which must be minimised to achieve a suitable degree of robustness. This is achieved using H_∞ optimisation given in the next section.
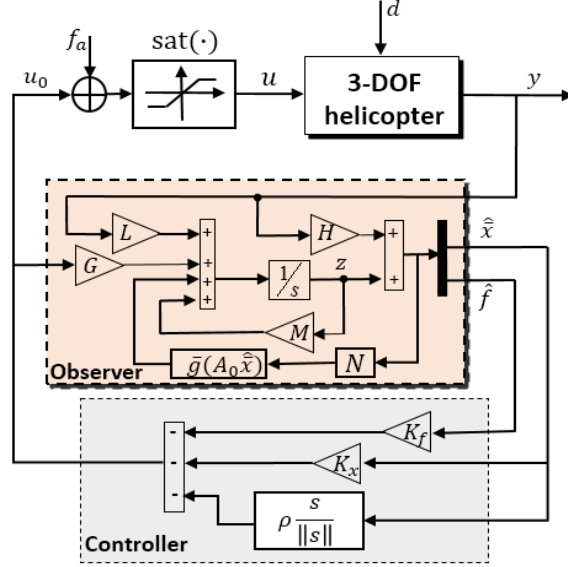
Fig. 3. *The proposed FE-based FTC 3-DOF helicopter system*

5. Synthesis of the FE observer and FTC controller

The 3-DOF helicopter FTC system (Fig. 3) includes the designs of the FE observer (9) and FTC controller (15). To obtain their gains, a way widely used in the literature is the separated FE/FTC design approach [23], in which the FE observer and FTC controller are designed separately. This approach follows the Separation Principle by neglecting of the effects of system uncertainty and nonlinearity on the FE performance and the effect of the estimation error on the FTC system. This section first presents the traditional separated synthesis approach with an analysis of its limitations, and then describes an approach based on the integrated FE/FTC strategy in [25], using the concept of bi-directional robustness interaction developed in the original work [24].

5.1. Traditional separated approach

By neglecting the effects of the system uncertainty and nonlinearity on the FE observer, the error system (12) is reduced to be

$$
\begin{aligned}
\dot{e} &= (\Xi\bar{A} - L_1\bar{C})e + \Xi\bar{D}\bar{d}_s, \\
z_{s_1} &= C_{s_1}e,
\end{aligned}
\tag{21}
$$

where $\bar{d}_s = [d_s^\top \ \dot{f}^\top]^\top$ and $d_s = [w_\varepsilon \ w_p]^\top$. $z_{s_1} \in \mathbb{R}^6$ is the measured output with a given coefficient matrix $C_{s_1} \in \mathbb{R}^{6\times 6}$.

The following theorem is given to design the matrices H and L_1 to make the error system (21) robustly asymptotically stable.

Theorem 2. Given a positive scalar γ_{s_1}, the error system (21) is asymptotically stable with H_∞ performance $\|G_{z_{s_1}\bar{d}_s}\|_\infty < \gamma_{s_1}$, if there exists a symmetric positive definite matrix $Q_s \in \mathbb{R}^{6\times 6}$, and

matrices $M_{s1} \in \mathbb{R}^{6 \times 4}$ and $M_{s2} \in \mathbb{R}^{6 \times 4}$ such that

$$
\begin{bmatrix}
\Omega_{1,1} & (Q_s - M_{s1}\bar{C})\bar{D} & C_{s1}^\top \\
\star & -\gamma_{s1}^2 I_4 & 0 \\
\star & \star & -I_6
\end{bmatrix} < 0,
$$

where $\Omega_{1,1} = \mathrm{He}\left(Q_s\bar{A} - M_{s1}\bar{C}\bar{A} - M_{s2}\bar{C}\right)$. Then the gains are given by $H = Q_s^{-1}M_{s1}$ and $L_1 = Q_s^{-1}M_{s2}$.

Proof. By using the Bounded Real Lemma [33] and defining $M_{s1} = Q_s H$ and $M_{s2} = Q_s L_1$, the proof is trivial and thus is omitted here. $\qquad\square$

Similarly, in the separated approach the FTC system is assumed to be not affected by the estimation error, thus the closed-loop control system (20) becomes

$$
\begin{aligned}
\dot{x} &= (\Theta A - BK_x)x + \Theta g(x) + \Theta D\tilde{d}, \\
z_{s_2} &= C_{s_2}x,
\end{aligned}
\tag{22}
$$

where $z_{s_2} \in \mathbb{R}^4$ is the measured output with a given coefficient matrix $C_{s_2} \in \mathbb{R}^{4 \times 4}$.

The following theorem is given to design K_x to ensure that (22) is robustly stable.

Theorem 3. Given positive scalars γ_{s_2} and ε_s, the closed-loop system (22) is asymptotically stable with H_∞ performance $\|G_{z_{s_2}\tilde{d}}\|_\infty < \gamma_{s_2}$, if there exists a symmetric positive definite matrix $P_s \in \mathbb{R}^{4 \times 4}$ and a matrix $M_{s3} \in \mathbb{R}^{2 \times 4}$ such that

$$
\begin{bmatrix}
\Pi_{1,1} & D & P_s C_{s_2}^\top & P_s \\
\star & -\gamma_{s_2}^2 I_2 & 0 & 0 \\
\star & \star & -I_4 & 0 \\
\star & \star & \star & -1/(\varepsilon_s L_f^2)I_4
\end{bmatrix} < 0,
$$

where $\Pi_{1,1} = \mathrm{He}(\Theta A P_s - B M_{s3}) + \varepsilon_s^{-1}\Theta\Theta^\top$. Then the control gain is given by $K_x = M_{s3}P_s^{-1}$.

Proof. See Appendix 10.1. $\qquad\square$

The separated approach outlined in Theorems 2 and 3 allows great design freedom for the FE/FTC design for the 3-DOF helicopter, in which the observer and controller can be optimised independently. However, when the obtained FE observer and FTC controller are implemented in the helicopter to formulate a closed-loop FTC system two problems arise: 1) The effects of the system uncertainty and nonlinearity on the observer are ignored in the design procedure, so in closed-loop operations the well designed observer is unable to achieve good estimation performance as expected; 2) Without taking the estimation error effect into account the control system will have slow transient performance with large overshoot and long settling time and compromised robustness. The above problems degrade the FE/FTC performance and can even result in an unstable FTC system.

It can be seen from the error system (12) and the control system (20) that the system uncertainty, nonlinearity and disturbance affect the estimation, and in turn the estimation error has an effect on the closed-loop control system. This leads to the fact that bi-directional robustness interactions exist between the FE and FTC functions, which breaks down the Separation Principle on which the separated approach based [24]. Therefore, it is necessary to introduce an integrated FE/FTC approach to achieve robust design of the overall FTC system, taking into account the bi-directional robustness interactions between the observer and controller.

5.2. Integrated approach

The composite closed-loop system encompassing (12) and (20) is

$$
\begin{aligned}
\dot{x} &= (\Theta_1 A - B K_x)x + B K e + \Theta g(x) + D_1 \bar{d}, \\
\dot{e} &= (\Xi \bar{A} - L_1 \bar{C})e + \Xi \Delta \bar{g} + \Xi \bar{D} \bar{d}, \\
z_c &= C_x x + C_e e,
\end{aligned}
\tag{23}
$$

where $z_c \in \mathbb{R}^4$ is the measured output used to verify the closed-loop system performance with matrices $C_x \in \mathbb{R}^{4\times4}$ and $C_e \in \mathbb{R}^{4\times6}$, and $D_1 = [\Theta D\ 0]$.

Theorem 4 provides an integrated strategy adopted from [25] to design the observer and controller gains simultaneously using a single-step LMI formulation .

Theorem 4. Given positive scalars γ, ε_1, ε_2, and ε_3, the closed-loop system (23) is asymptotically stable with H_∞ performance $\|G_{z_c\bar{d}}\|_\infty < \gamma$, if there exist three symmetric positive definite matrices $Z \in \mathbb{R}^{4\times4}$, $Q \in \mathbb{R}^{4\times4}$, and $R \in \mathbb{R}^{2\times2}$, and matrices $M_1 \in \mathbb{R}^{2\times4}$, $M_2 \in \mathbb{R}^{4\times2}$, $M_3 \in \mathbb{R}^{4\times2}$, $M_4 \in \mathbb{R}^{2\times4}$, and $M_5 \in \mathbb{R}^{2\times4}$ such that

$$
\begin{bmatrix} \Pi_1 & \Pi_2 \\ \star & \Pi_3 \end{bmatrix} < 0,
\tag{24}
$$

with

$$
\begin{aligned}
\Pi_1 &= \begin{bmatrix} \Xi_{1,1} & \Xi_{1,2} \\ \star & J_{2,2} \end{bmatrix}, \\
\Pi_2 &= \begin{bmatrix} \Xi_{1,3} & \Xi_{1,4} & \Xi_{1,5} & 0 & 0 & \Xi_{1,8} \\ J_{2,3} & J_{2,4} & 0 & I_4 & J_{2,7} & 0 \end{bmatrix}, \\
\Pi_3 &= -\mathrm{diag}\left\{ \gamma^2 I_4, I_4, \varepsilon_3^{-1}Z, \varepsilon_3 Z, \varepsilon_1 I_4, (\varepsilon_2 L_f^2)^{-1}I_4 \right\}, \\
J_{2,2} &= \begin{bmatrix} \Xi_{2,2} & \Xi_{2,3} \\ \star & \Xi_{3,3} \end{bmatrix}, \quad J_{2,3} = \begin{bmatrix} QD - M_2 CD & 0 \\ -M_4 CD & R \end{bmatrix}, \\
J_{2,4} &= C_e^\top = \begin{bmatrix} C_{ex}^\top \\ C_{ef}^\top \end{bmatrix}, \quad J_{2,7} = \begin{bmatrix} Q - M_2 C & 0 \\ -M_4 C & R \end{bmatrix}, \\
\Xi_{1,1} &= \mathrm{He}(\Theta A Z - B M_1) + \varepsilon_2^{-1}\Theta\Theta^\top, \Xi_{1,2} = [0\ B], \\
\Xi_{1,3} &= [\Theta D\ 0],\ \Xi_{1,4} = Z C_x^\top,\ \Xi_{1,5} = B M_1,\ \Xi_{1,8} = Z, \\
\Xi_{2,2} &= \mathrm{He}(QA - M_2 CA - M_3 C) + \varepsilon_1 L_f^2 I_4, \\
\Xi_{2,3} &= QB - M_2 CB - A^\top C^\top M_4^\top - C^\top M_5^\top, \\
\Xi_{3,3} &= \mathrm{He}(-M_4 CB).
\end{aligned}
$$

Then the controller gains are given by: $K_x = M_1 Z^{-1}$, $H_1 = Q^{-1}M_2$, $H_2 = R^{-1}M_4$, $L_{11} = Q^{-1}M_3$, $L_{12} = R^{-1}M_5$.

Proof. See Appendix 10.2. $\qquad\square$

Remark 4. The inequalities in Theorems 2 - 4 are solved using the Matlab LMI toolbox [34], after choosing the following parameters: 1) H_∞ performance indices γ_{s1}, γ_{s2}, and γ, which are positive scalars that normally chosen within $[0, 1]$ to attenuate the disturbance effect; 2) Other parameters ε_s, ε_1, ε_2, and ε_3, which are positive scalars introduced to offer more design freedom to handle the

nonlinearity. However, they affect the obtained observer and controller gains and subsequently the FE and FTC system performance. The constraints listed above can be a guidance which makes it usually rather easy to find a suitable set of parameters to achieve admissible system stability and asymptotic estimation and fault-tolerant control performance. Hence, in reality these parameters are chosen through trial and error.

Remark 5. In the presence of actuator faults, the proposed strategy estimates and compensates the total effect of the actuator faults and saturation and robustly recover the normal non-saturated system performance. In the fault-free cases, it can be used as a novel anti-windup control framework to recover non-saturated system performance. Adaptive anti-windup controls have been described in many works, e.g., [35], by incorporating an auxiliary system. Nevertheless, this adaptive framework involves a switched designed control through appropriately chosen bounds of the auxiliary system state. Other mainstream anti-windup methods incorporate anti-windup compensators as a part of the normal control function, as summarized in the review [36]. However, the above anti-windup designs are implemented with the measurement of the actuator output, which is not the case in reality and is not even desirable, especially if the actuator has any fast, unmodeled dynamics. Compared with the existing approaches, the proposed design for anti-windup control is convenient in the sense that 1) the proposed observer can achieve simultaneous estimation of the system state and saturation effect without requiring the actuator output measurement, and 2) all the observer and controller gains are obtained by solving the LMI (24) in a single-step.

6. Simulation results

This section outlines comparative simulations for the elevation and pitch motions of the Quanser 3-DOF helicopter system (5) with single or multiple actuator faults, using 1) the nominal control design (without FE/FTC and the state observer and controller are designed separately), 2) the separated FE/FTC approach, and 3) the proposed integrated FE/FTC approach.

Table 2 Parameters of the 3-DOF helicopter system

Parameter	Value
J_ε	$0.91 \ \text{kg} \cdot \text{m}^2$
J_p	$0.0364 \ \text{kg} \cdot \text{m}^2$
K_f	$0.5 \ \text{N/V}$
m_h	$1.01 \ \text{kg}$
L_a	$0.66 \ \text{m}$
L_h	$0.177 \ \text{m}$
g	$9.81 \ \text{m/s}^2$

The 3-DOF helicopter system parameters are given in Table 2. Due to mechanical limits, the elevation angle is constrained within the range of $\pm 31.75 \deg$ and the pitch angle is within $\pm 32 \deg$. The voltage limits of the front and back motors are $\pm 12 \ \text{V}$. The external disturbances acting on the helicopter are supposed to be $w_\varepsilon = 0.01 \sin(10t)$ and $w_p = 0.01 \sin(5t)$. To test the system performance, a Gaussian noise with zero-mean and variance 0.001^2 is added to the output measurement.

Choosing $Y_1 = 0.1_{2 \times 4}$, $C_x = I_4$, $C_e = [C_{ex} \ C_{ef}] = [I_4 \ 1_{4 \times 2}]$, and solving Theorem 4 with $\varepsilon_1 = 50$, $\varepsilon_2 = 5$, $\varepsilon_3 = 0.015$, and $\gamma = 1$, gives the following observer and controller gains:

$$N_1 = \begin{bmatrix} -0.1 & -0.1 & 1.3788 & 0.2056 \\ -0.1 & -0.1 & 1.3788 & -0.2056 \end{bmatrix},$$

13

$$K_x = \begin{bmatrix} 9.7303 & 1.3552 & 9.1113 & 1.3457 \\ 9.7384 & -1.5439 & 9.1113 & -1.3540 \end{bmatrix},$$

$$M = \begin{bmatrix} -1.4142 & 0 & 0 & 0 & 0 & 0 \\ 0 & -1.4142 & 0 & 0 & 0 & 0 \\ 0 & 0 & -1.4142 & 0 & 0 & 0 \\ 0 & 0 & 0 & -1.4142 & 0 & 0 \\ -0.9026 & -0.9016 & -0.8991 & -0.8981 & -27.5619 & 16.6599 \\ -0.9025 & -0.9034 & -0.8991 & -0.9068 & 16.6545 & -27.55631 \end{bmatrix},$$

$$N = \begin{bmatrix} 0 & 0 & 0 & 0 & 0 & 0 \\ 0 & 0 & 0 & 0 & 0 & 0 \\ 0 & 0 & 0 & 0 & 0 & 0 \\ 0 & 0 & 0 & 0 & 0 & 0 \\ -0.0004 & -0.0013 & -15.0315 & -9.0942 & 1 & 0 \\ -0.0004 & 0.0013 & -15.0312 & 9.0919 & 0 & 1 \end{bmatrix},$$

$$G = \begin{bmatrix} 0 & 0 \\ 0 & 0 \\ 0 & 0 \\ 0 & 0 \\ -27.5619 & 16.6599 \\ 16.6545 & -27.5563 \end{bmatrix},$$

$$L = \begin{bmatrix} 0 & 0 & 0 & 0 \\ 0 & 0 & 0 & 0 \\ 0 & 0 & 0 & 0 \\ 0 & 0 & 0 & 0 \\ -0.0042 & -0.0579 & -163.8797 & -402.1261 \\ -0.0042 & 0.0579 & -163.8614 & 402.0014 \end{bmatrix},$$

$$H = \begin{bmatrix} 1 & 0 & 0 & 0 \\ 0 & 1 & 0 & 0 \\ 0 & 0 & 1 & 0 \\ 0 & 0 & 0 & 1 \\ 0.0004 & 0.0013 & 15.0315 & 9.0942 \\ 0.0004 & -0.0013 & 15.0312 & -9.0919 \end{bmatrix}.$$

The other control parameters are chosen as: $\phi = 0.4$, $\varphi = 7.6$, $\epsilon = 0.1$, $\sigma = 0.01$, and $\theta_0 = 0.001$.

For the separated design, the observer and controller gains are obtained by solving the LMIs in Theorems 2 and 3 with $\gamma_{s_1} = 0.55$, $\gamma_{s_2} = 0.7$, and $\varepsilon_s = 0.01$.

All the three cases are simulated with $\varepsilon(0) = 30$ deg and $p(0) = 18$ deg, and the initial values of other parameters are all set to zero. A first-order low pass filter, whose transfer function is $1/(2\pi f_0 s + 1)$ with a frequency $f_0 = 7$ Hz, is used to filter each of the measure outputs.

6.1. Case 1: fault-free

In this case the separated and integrated FE/FTC designs revert to nominal observer-based state feedback robust controls. It is seen from Fig. 4 that all of the three control approaches can stabilise the elevation and pitch angles with similar control efforts. However, the proposed integrated design has the best transient angle responses.
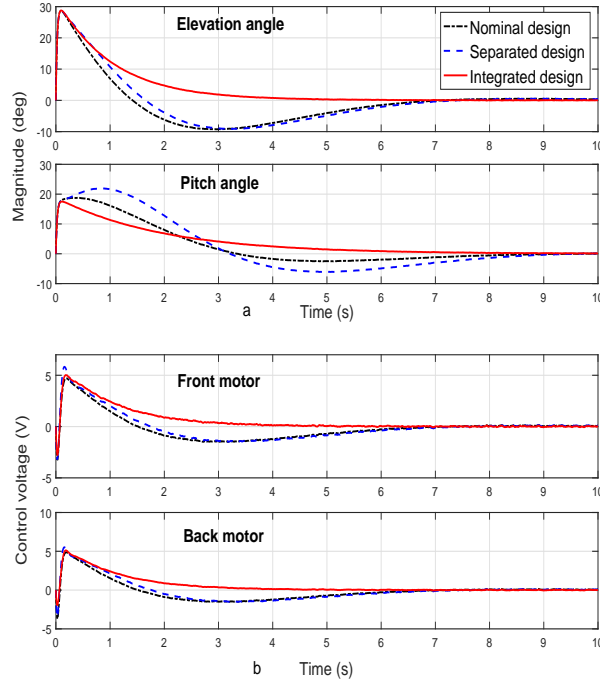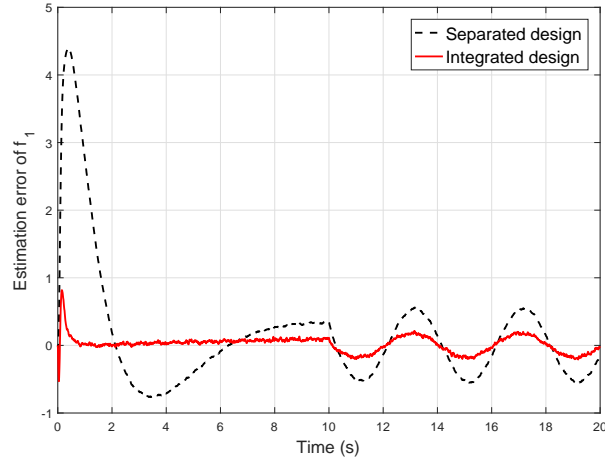

Fig. 4. *Angle response and control effort: Case 1. (a) Angle response; (b) Control effort*

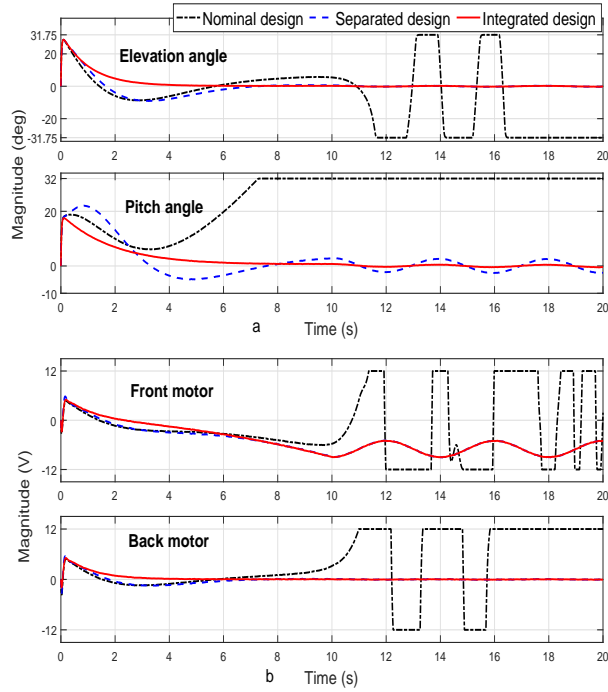## 6.2. Case 2: single actuator fault

In this case the back actuator of the helicopter is healthy, while the front actuator has an actuator fault characterized by

$$f_{a1}(t) = \begin{cases} 0.1t + 0.08t^2, & 0 \text{ s} \leq t \leq 10 \text{ s} \\ 2\cos(0.5\pi(t-10)) + 7, & 10 \text{ s} < t \leq 20 \text{ s} \end{cases}.$$

It is shown in Fig. 5 that the proposed integrated design has better FE performance than the separated design. The angle responses and control efforts in Fig. 6 show that only the proposed integrated design can stabilise both the elevation and pitch angles in the presence of a single actuator fault. The separated design stabilises the elevation angle but has oscillatory pitch angle response. The nominal design suffers from saturations in the angles and control inputs.

15

Fig. 5. *Fault estimation performance: Case 2*

Fig. 6. *Angle response and control effort: Case 2. (a) Angle response; (b) Control effort*

6.3. Case 3: multiple actuator faults

In this case the front and back actuators have oscillatory faults f_{a1} and f_{a2}, respectively. The faults are characterized by

$$f_{a1}(t) = \begin{cases} 0.1t + 0.08t^2, & 0\text{ s} \le t \le 10\text{ s} \\ 2\cos(0.5\pi(t-10)) + 7, & 10\text{ s} < t \le 20\text{ s} \end{cases},$$

$$f_{a2}(t) = \sin(0.5t) + 0.5\sin(t), \ 0\text{ s} \le t \le 20\text{ s}.$$

16

Similar to Case 2, the results in Figs. 7 - 8 show that compared with the other two approaches, the proposed integrated approach achieves better performances of FE and output stabilisation. Moreover, the nominal design has saturations in the angles and control inputs, while the separated design suffers from significant oscillation in the pitch angle response.
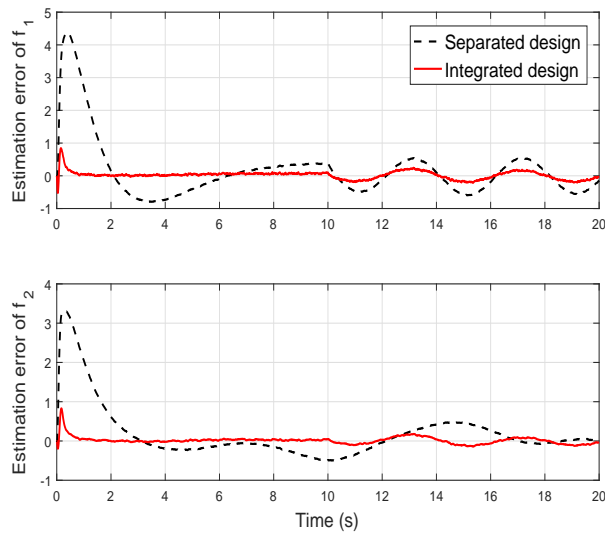
Fig. 7. *Fault estimation performance: Case 3*
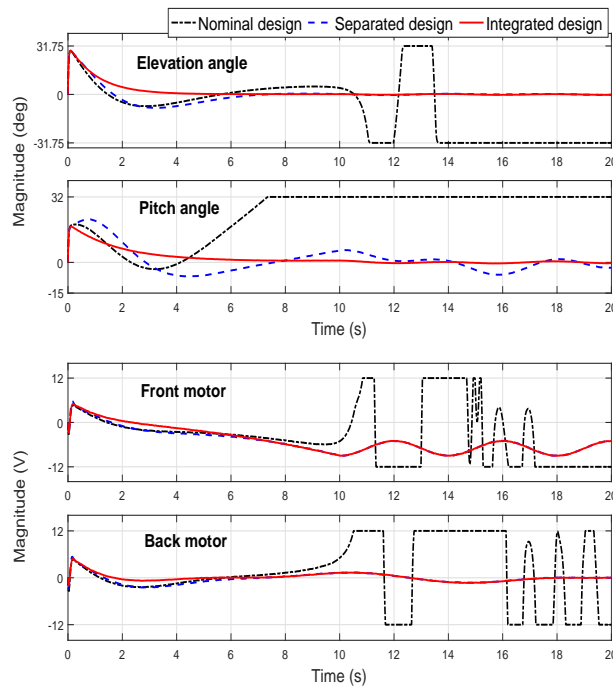
Fig. 8. *Angle response and control effort: Case 3. (a) Angle response; (b) Control effort*

Summarizing the results of the three simulation cases: 1) Compared with the nominal and separated designs, the proposed integrated design stabilises the elevation and pitch motions of

the 3-DOF helicopter system with the best transient performance and meanwhile avoids actuator saturation, no matter if actuator faults exist or not. Although the separated design can also avoid actuator saturation in the presence of actuator faults, it suffers from pitch angle oscillation. 2) The proposed integrated design approach achieves more accurate fault estimation than the separated design.

The results represent well the expected behaviour of the FTC cases, since 1) the nominal design does not include FE and FTC modules, and 2) the separated design neglects the bi-directional robustness interactions between the FE observer and FTC system, resulting from inaccurate estimation as well as system performance with low robustness.

7. Conclusion

An FE-based FTC design has been proposed for a nonlinear 3-DOF helicopter system subject to actuator faults, saturation and system uncertainty along with external disturbance. Furthermore, the work is a realistic laboratory application study with some dynamic characteristics typical of the rigid body motions of a tandem rotor helicopter. A NUIO is used to estimate the system state and a composite fault function of the actuator faults and saturation. An adaptive sliding mode FTC controller using the estimates is designed to compensate the fault and saturation effects and achieve robust stabilisation of the elevation and pitch motions. An integrated design approach described in earlier papers by the authors makes use of a single-step LMI formulation to solve the observer and controller gains, accounting for the bi-directional robustness interactions between the FE and FTC functions. The earlier research did not consider the important effect of the actuator saturation. Hence, the novelty lies in the inclusion of both actuator faults (oscillation and drift) as well as saturation as an additional hard nonlinearity. Results are compared with the nominal control (with no applied FTC action) as well as with the more traditional approach to combined FE and FTC using separated FE/FTC designs. The proposed integrated approach is demonstrated as a more effective design for attaining robust FTC performance (stabilisation and fault compensation). Future research will focus on the control of all the three motions of a helicopter system.

8. Acknowledgement

9. References

[1] Edwards, C., Lombaerts, T., Smaili, H.: 'Fault Tolerant Flight Control: A Benchmark Challenge'. vol. 399. (Springer Science & Business Media, 2010)

[2] Zolghadri, A., Henry, D., Cieslak, J., Efimov, D., Goupil, P.: 'Fault Diagnosis and Fult-tolerant Control and Guidance for Aerospace Vehicles'. (Springer, 2014)

[3] Patton, R.J. 'Fault-tolerant control'. In: Encyclopedia of Systems and Control. (Springer, 2015. pp. 422–428

[4] Hua, M.D., Hamel, T., Morin, P., Samson, C.: 'Introduction to feedback control of underactuated VTOL vehicles: a review of basic control design ideas and principles', *IEEE Contr. Syst. Mag.*, 2013, **33**, (1), pp. 61–75

[5] Chen, M., Ge, S., Ren, B.: 'Robust attitude control of helicopters with actuator dynamics using neural networks', *IET Control Theory Appl.*, 2010, **4**, (12), pp. 2837–2854

[6] Alexis, K., Nikolakopoulos, G., Tzes, A.: 'Model predictive quadrotor control: attitude, altitude and position experimental studies', *IET Control Theory Appl.*, 2012, **6**, (12), pp. 1812–1827

[7] Li, Z., Yu, J., Xing, X., Gao, H.: 'Robust output-feedback attitude control of a three-degree-of-freedom helicopter via sliding-mode observation technique', *IET Control Theory Appl.*, 2015, **9**, (11), pp. 1637–1643

[8] Izaguirre.Espinosa, C., Muñoz.Vázquez, A.J., Sánchez.Orta, A., Parra.Vega, V., Castillo, P.: 'Attitude control of quadrotors based on fractional sliding modes: theory and experiments', *IET Control Theory Appl.*, 2016, **10**, (7), pp. 825–832

[9] Vachtsevanos, G., Tang, L., Drozeski, G., Gutierrez, L.: 'From mission planning to flight control of unmanned aerial vehicles: strategies and implementation tools', *Annu. Rev. Control*, 2005, **29**, (1), pp. 101–115

[10] Ducard, G.J.: 'Fault-tolerant Flight Control and Guidance Systems: Practical Methods for Small Unmanned Aerial Vehicles'. (Springer Science & Business Media, 2009)

[11] Qi, X., Theilliol, D., Qi, J., Zhang, Y., Han, J., Song, D., et al. 'Fault diagnosis and fault tolerant control methods for manned and unmanned helicopters: a literature review'. In: Proc. SysTol. (IEEE, 2013. pp. 132–139

[12] Valavanis, K.P., Vachtsevanos, G.J.: 'Handbook of Unmanned Aerial Vehicles'. (Springer Publishing Company, Incorporated, 2014)

[13] Qi, X., Qi, J., Theilliol, D., Zhang, Y., Han, J., Song, D., et al.: 'A review on fault diagnosis and fault tolerant control methods for single-rotor aerial vehicles', *J. Intell. Robot. Syst.*, 2014, **73**, (1-4), pp. 535–555

[14] Apkarian, J.: '3-DOF helicopter reference manual', *Quanser Consulting Inc, Canada*, 2006,

[15] Shan, J., Liu, H.T., Nowotny, S.: 'Synchronised trajectory-tracking control of multiple 3-DOF experimental helicopters', *IET Control Theory Appl.*, 2005, **152**, (6), pp. 683–692

[16] Zheng, B., Zhong, Y.: 'Robust attitude regulation of a 3-DOF helicopter benchmark: theory and experiments', *IEEE Trans. Ind. Electron.*, 2011, **58**, (2), pp. 660–670

[17] Meza.Sánchez, M., Aguilar, L.T., Orlov, Y.: 'Output sliding mode-based stabilization of underactuated 3-DOF helicopter prototype and its experimental verification', *J. Franklin Inst.*, 2015, **352**, (4), pp. 1580–1594

[18] Chen, F., Zhang, K., Jiang, B., Wen, C.: 'Adaptive sliding mode observer-based robust fault reconstruction for a helicopter with actuator fault', *Asian J. Control*, 2016, **18**, (4), pp. 1558–1565

[19] Afonso, R.J.M., Galvão, R.K.H. 'Predictive control of a helicopter model with tolerance to actuator faults'. In: Proc. SysTol. (IEEE, 2010. pp. 744–751

[20] Chen, F., Hou, R., Jiang, B., Tao, G.: 'Study on fast terminal sliding mode control for a helicopter via quantum information technique and nonlinear fault observer', *Int. J. Innovative Comput. Inf. Control*, 2013, **9**, (8), pp. 3437–3447

[21] Wang, Z., Chen, F., Jiang, B. 'An improved nonlinear model and adaptive fault-tolerant control for a twin rotor helicopter'. In: Proc. 33rd Chinese Control Conf. (IEEE, 2014. pp. 3208–3212

[22] Chen, M., Shi, P., Lim, C.C.: 'Adaptive neural fault-tolerant control of a 3-DOF model helicopter system', *IEEE Trans. Syst., Man, Cybern., Syst.*, 2016, **46**, (2), pp. 260–270

[23] de Loza, A.F., Cieslak, J., Henry, D., Zolghadri, A., Fridman, L.M.: 'Output tracking of systems subjected to perturbations and a class of actuator faults based on HOSM observation and identification', *Automatica*, 2015, **59**, pp. 200–205

[24] Lan, J., Patton, R.J.: 'A new strategy for integration of fault estimation within fault-tolerant control', *Automatica*, 2016, **69**, pp. 48–59

[25] Lan, J., Patton, R.J.: 'Integrated fault estimation and fault-tolerant control for uncertain Lipschitz nonlinear systems', *Int. J. Robust Nonlin.*, DOI: 10.1002/rnc.3597, 2016,

[26] Kiefer, T., Graichen, K., Kugi, A.: 'Trajectory tracking of a 3-DOF laboratory helicopter under input and state constraints', *IEEE Trans. Control Syst. Technol.*, 2010, **18**, (4), pp. 944–952

[27] Zheng, Z., Sun, L., Zou, Y. 'Attitude tracking control of a 3-DOF helicopter with actuator saturation and model uncertainties'. In: Proc. 34th Chinese Control Conf. (IEEE, 2015. pp. 5641–5646

[28] Edwards, C., Spurgeon, S.: 'Sliding Mode Control: Theory and Applications'. (CRC Press, 1998)

[29] Goupil, P.: 'Oscillatory failure case detection in the A380 electrical flight control system by analytical redundancy', *Control Eng. Pract.*, 2010, **18**, (9), pp. 1110–1119

[30] Li, Y.X., Yang, G.H.: 'Adaptive fuzzy decentralized control for a class of large-scale nonlinear systems with actuator faults and unknown dead zones', *IEEE Trans. Syst., Man, Cybern., Syst.*, DOI: 10.1109/TSMC.2016.2521824, 2016,

[31] Li, Y.X., Yang, G.H.: 'Robust adaptive fault-tolerant control for a class of uncertain nonlinear time delay systems', *IEEE Trans. Syst., Man, Cybern., Syst.*, DOI: 10.1109/TSMC.2016.2634080, 2016,

[32] Freidovich, L.B., Khalil, H.K.: 'Performance recovery of feedback-linearization-based designs', *IEEE Trans. Autom. Control*, 2008, **53**, (10), pp. 2324–2334

[33] Zhou, K., Doyle, J.C., Glover, K.: 'Robust and Optimal Control'. vol. 40. (Prentice Hall New Jersey, 1996)

[34] Gahinet, P., Nemirovskii, A., Laub, A.J., Chilali, M. 'The LMI control toolbox'. In: Proc. IEEE Conf. Decis. Control. vol. 3. (IEEE, 1994. pp. 2038–2041

[35] He, W., Dong, Y., Sun, C.: 'Adaptive neural impedance control of a robotic manipulator with input saturation', *IEEE Trans. Syst., Man, Cybern., Syst.*, 2016, **46**, (3), pp. 334–344

[36] Tarbouriech, S., Turner, M.: 'Anti-windup design: an overview of some recent advances and open problems', *IET Control Theory Appl.*, 2009, **3**, (1), pp. 1–19

[37] Boyd, S.P., El.Ghaoui, L., Feron, E., Balakrishnan, V.: 'Linear Matrix Inequalities in System and Control Theory'. vol. 15. (SIAM, 1994)

10. Appendices

10.1. Proof of Theorem 3

Given a symmetric positive definite matrix $Z_s \in \mathbb{R}^{4\times 4}$. Assume $g(0) = 0$, then $\|g(x)\| \leq L_f\|x\|, \forall x \in \mathbb{R}^4$. Thus for some positive scalar ε_s,

$$2x^\top Z_s \Theta g(x) \leq \varepsilon_s^{-1} x^\top Z_s \Theta \Theta^\top Z_s x + \varepsilon_s L_f^2 \|x\|^2.$$

Using the Bounded Real Lemma, the closed-loop system (22) is stable with H_∞ performance $\|G_{z_{s_2}\tilde{d}}\|_\infty < \gamma_{s_2}$, if

$$\begin{bmatrix} \Pi_{1,1} & Z_s D & C_{s_2}^\top \\ \star & -\gamma_{s_2}^2 I_2 & 0 \\ \star & \star & -I_4 \end{bmatrix} < 0, \tag{25}$$

where $\Pi_{1,1} = \mathrm{He}\left[Z_s(\Theta A - BK_x)\right] + \varepsilon_s^{-1} Z_s \Theta \Theta^\top Z_s + \varepsilon_s L_f^2 I_4$.

Define $P_s = Z_s^{-1}$ and $M_{s3} = K_x P_s$. Pre- and post-multiplying both sides of (25) with $\mathrm{diag}(P_s, I_2, I_4)$ and using the Schur complement [37], then (25) becomes

$$\begin{bmatrix} \Pi_{1,1} & D & P_s C_{s_2}^\top & P_s \\ \star & -\gamma_{s_2}^2 I_2 & 0 & 0 \\ \star & \star & -I_4 & 0 \\ \star & \star & \star & -1/(\varepsilon_s L_f^2)I_4 \end{bmatrix} < 0,$$

where $\Pi_{1,1} = \mathrm{He}(\Theta A P_s - BM_{s3}) + \varepsilon_s^{-1}\Theta\Theta^\top$.

10.2. Proof of Theorem 4

Define a symmetric positive definite matrix $P_1 \in \mathbb{R}^{6\times 6}$. Since the nonlinear function $g(x)$ is Lipschitz, for some positive scalar ε_1,

$$2e^\top P_1 \Xi \Delta \bar{g} \leq \varepsilon_1^{-1} e^\top P_1 \Xi \Xi^\top P_1 e + \varepsilon_1 L_f^2 \|A_0 e\|^2.$$

Define another symmetric positive definite matrix $P \in \mathbb{R}^{4\times 4}$. Assume $g(0) = 0$, then $\|g(x)\| \leq L_f\|x\|, \forall x \in \mathbb{R}^4$. It thus holds that, for some positive scalar ε_2,

$$2x^\top P\Theta g(x) \leq \varepsilon_2^{-1} x^\top P\Theta\Theta^\top Px + \varepsilon_2 L_f^2 \|x\|^2.$$

Using the Bounded Real Lemma, the closed-loop system (20) is stable with H_∞ performance $\|G_{z_c\bar{d}}\|_\infty < \gamma$ if

$$
\begin{bmatrix}
J_{1,1} & PBK & PD_1 & C_x^\top \\
\star & J_{2,2} & P_1\Xi\bar{D} & C_e^\top \\
\star & \star & -\gamma^2 I_4 & 0 \\
\star & \star & \star & -I_4
\end{bmatrix} < 0,
\tag{26}
$$

where $J_{1,1} = \mathrm{He}\left[P(\Theta A - BK_x)\right] + \varepsilon_2^{-1}P\Theta\Theta^\top P + \varepsilon_2 L_f^2 I_4$ and $J_{2,2} = \mathrm{He}\left[P_1(\Xi\bar{A} - L_1\bar{C})\right] + \varepsilon_1^{-1}P_1\Xi\Xi^\top P_1 + \varepsilon_1 L_f^2 A_0^\top A_0 I_6$.

Define $Z = P^{-1}$. Pre- and post-multiplying both sides of (26) with $\mathrm{diag}(Z, I_6, I_4)$ gives

$$
\begin{bmatrix}
J_{1,1} & BK & D_1 & ZC_x^\top \\
\star & J_{22} & P_1\Xi\bar{D} & C_e^\top \\
\star & \star & -\gamma^2 I_4 & 0 \\
\star & \star & \star & -I_4
\end{bmatrix} < 0,
\tag{27}
$$

where $J_{1,1} = \mathrm{He}\left[(\Theta A - BK_x)Z\right] + \varepsilon_2^{-1}\Theta\Theta^\top + \varepsilon_2 L_f^2 ZZ$ and $J_{2,2} = \mathrm{He}\left[P_1(\Xi\bar{A} - L_1\bar{C})\right] + \varepsilon_1^{-1}P_1\Xi\Xi^\top P_1 + \varepsilon_1 L_f^2 A_0^\top A_0 I_6$.

By the Young relation [37], for some positive scalar ε_3,

$$
\mathrm{He}\left\{\Gamma_1\Gamma_2^\top\right\} \le \varepsilon_3\Gamma_1 Z^{-1}\Gamma_1^\top + \varepsilon_3^{-1}\Gamma_2 Z^{-1}\Gamma_2^\top,
$$

$$
\Gamma_1 = \begin{bmatrix} BK_x Z \\ 0 \\ 0 \end{bmatrix}, \ \Gamma_2 = \begin{bmatrix} 0 \\ I_4 \\ 0 \end{bmatrix}.
$$

Further define $P_1 = \mathrm{diag}(Q_{4\times4}, R_{2\times2})$, $L_1 = [L_{11}; L_{12}]$, $H = [H_1; H_2]$, $M_1 = K_x Z$, $M_2 = QH_1$, $M_3 = QL_{11}$, $M_4 = RH_2$, and $M_5 = RL_{12}$. Using the Schur complement repeatedly, (27) can be finally reformulated into (24).